Appl Biochem Biotechnol (2009) 152:29–41
DOI 10.1007/s12010-008-8204-5

Deactivation Kinetics and Response Surface Analysis of the Stability of α-L-Rhamnosidase from *Penicillium decumbens*

I. Magario · A. Neumann · E. Oliveros · C. Syldatk

Received: 2 November 2007 / Accepted: 24 January 2008 /
Published online: 27 August 2008

Abstract The stability of the mixed enzyme preparation Naringinase from *Penicillium decumbens* was studied in dependence of the temperature, the pH value, and the enzyme concentration by means of response surface methodology. Deactivation kinetics by formation of an intermediate state was proposed for fitting deactivation data. Empirical models could then be constructed for prediction of deactivation rate constants, specific activity of intermediate state, and half-life values under different incubation conditions. From this study, it can be concluded that (1) Naringinase is most stable in the pH range of 4.5–5.0, being quite sensitive to lower pHs (<3.5) and (2) the glyco-enzyme is a rather thermo-stable enzyme preserving its initial activity for long times when incubated at its optimal pH up to temperatures of 65 °C. Enriched α-L-rhamnosidase after column treatment and ultrafiltration presented similar deactivation kinetics pattern and half-life values as the unpurified enzyme. Thus, any influence of low molecular weight substances on its deactivation is most probably negligible. The intermediate state of the enzyme may correspond to unfolding and self-digestion of its carbohydrate portion, lowering its activity relative to the initial state. The digestion- and unfolding-grade of this intermediate state may also be controlled by the pH and temperature of incubation.

Keywords Naringinase · Doehlert array · Response surface methodology · Series-type deactivation kinetics · α-Rhamnosidase · Enzyme stability

I. Magario (✉) · A. Neumann · C. Syldatk
Institute of Engineering in Life Sciences, Chair of Technical Biology, University of Karlsruhe (TH), Engler-Bunte-Ring 1, 76128 Karlsruhe, Germany
e-mail: Ivana.Magario@tebi.uni-kalrsruhe.de

E. Oliveros
Lehrstuhl für Umweltmesstechnik, Engler-Bunte-Institut, Universität Karlsruhe, Engler-Bunte-Ring 1, 76128 Karlsruhe, Germany
e-mail: oliveros@chimie.ups-tlse.fr

Present address:
E. Oliveros
Laboratoire des IMRCP, UMR CNRS 5623, Université Paul Sabatier, 31062 Toulouse cédex 9, France

Introduction

Naringinase is an enzyme complex consisting of α-L-rhamnosidase (EC 3.2.1.40) and β-glucosidase (EC 3.2.1.21) [1–5]. Historically, its production and major application was targeted for the debittering of citrus juices. Indeed, α-L-rhamnosidase converts the bitter glycoside naringin to the less-bitter prunin by cleavage of an α-(1→2) bond between L-rhamnose and glucose. Subsequent hydrolysis of glucose from prunin by the β-glucosidase portion yields finally the aglycone naringenin. The α-L-rhamnosidase activity of Naringinase finds further applications in the production of prunin, for aroma enhancement of wine, in steroid transformation, in the structural study of bacterial polysaccharide, and in the production of L-rhamnose from glycosides [2, 6–9]. Furthermore, *Penicillium*-α-L-rhamnosidases are known to be capable of hydrolysing L-rhamnose from rhamnolipids [10, 11]. Meiwess et al. [11] reported that a commercial *Penicillium*-Naringinase was able to cleave quantitatively the glycosidic bond between the two L-rhamnose units of dirhamnolipids. The subsequent bond cleavage between L-rhamnose and the (*R*,*R*)-3-(3-hydroxydecanoyloxy)decanoic acid portion of the resulted monorhamnolipid was also achieved, however, at rather low rates.

α-L-Rhamnosidases are mainly produced by the fungal species *Aspergillus* and *Penicillium* [1, 2, 6–8, 10, 12–16], whereas bacterial and plant sources are also reported. α-L-Rhamnosidase from *Penicillium decumbens* is an extracellular glycoprotein (50% glycosidation grade) of 90 kDa showing optimal activity at pH 3.5–4.5 and 57 °C [3, 17]. In contrast to the other fungal α-L-rhamnosidases, less information is published about its stability profiles of the free form, and most studies deal with stabilities in immobilized state [18–21].

For optimization of enzymatic processes, not only high activities but also high stabilities of the catalyst are desirable [22]. It is well known that temperature is the most important variable affecting enzyme deactivation by weakening non-covalent interactions that stabilize the protein structure, leading to unfolding and subsequent changes that reduce the catalytic activity [23]. Variation in the pH value can also irreversibly change this delicate structure by alteration of the charge of the amino acid responsible for maintenance of the secondary and tertiary structure [24]. Extreme pH values lead similarly to chemical modification fully inactivating the enzyme. Enzyme concentration is also known to affect inactivation by modifying aggregation and subunit dissociation grade [23]. There are many examples of enhanced stabilities at high enzyme concentrations [5, 25].

The objective of this study was to quantify the effect of temperature, pH, and enzyme concentration on *Penicillium*-α-L-rhamnosidase stability for a rational selection of process conditions in view of its promising application for enzymatic modification of rhamnolipids. For that, optimal experimental design techniques were applied for collecting stabilization data in a minimum set of optimal-located experimental points for building of a response surface model. The efficiency of the technique for enzyme stability studies was demonstrated.

Materials and Methods

Enzyme and Chemicals

Naringinase from *P. decumbens* was purchased from Sigma Aldrich (Steinheim, Germany) (Lot 110K16471, 511 U g^{-1} Naringinase or α-L-rhamnosidase activity, and 55 U g^{-1} β-glucosidase activity). The model substrate *p*-nitrophenyl-α-L-rhamnoside (pnpR) used for

activity assays was obtained from Extrasynthese (Genay, France). All other chemicals were of analytical grade.

Experimental Procedure

Enzyme Stability Assay

Different enzyme solutions were incubated in plastic cups at controlled temperature under 1,400 rpm agitation in a thermoblock unit. At different times, aliquots were withdrawn, and the enzyme activity was immediately measured. For the determination of initial enzyme activity, a first sampling at room temperature before incubation was carried out. Incubation buffers (0.1 M) were as follows: sodium formate for pH 2.50–3.38, sodium acetate for pH 4.25–5.13, and sodium phosphate for pH 6.00. Naringinase stability tests at low concentration were carried out at pH 5.5 and 40–60 °C and a Naringinase powder concentration of 0.01 g l^{-1}. For avoiding protein adsorption on the vessel walls, plastic cups were pre-treated by incubation of a bovine serum albumin (BSA) or Naringinase solution into them. Incubation was conducted at 1 g l^{-1} powder concentration in sodium acetate buffer pH 5.5, 60°C, and 1,400 rpm for 1 h.

Enzyme Enrichment

Enrichment of α-L-rhamnosidase from the commercial powder was carried out with an ÄKTAexplorer equipment coupled to a control system (Unicorn; Amersham Biosciences, Uppsala, Sweden). For selection of running buffer pH, small scale assay were carried out on a 1 ml-Hitrap-Q-FF column (Amersham Biosciences) with different equilibration buffers: 50 mM Tris–HCl for pH 7.5 and 7.0 and 50 mM potassium phosphate for pH 6.5. Larger protein amounts (5 g Naringinase powder equivalent to 0.4 g protein) were applied on a 20 ml Hiload Q-sepharose HP (Amersham Biosciences) column and eluted in 50 mM potassium phosphate buffer for pH 6.5 at 4 ml min^{-1} after 12-column volume (CV) equilibration time with a 40 CV linear gradient from 0 to 0.5 M potassium chloride. Fractions containing α-L-rhamnosidase were pooled, desalted, and concentrated in a stirred ultrafiltration cell (Amicon Inc., Beverly, USA) with a 30-kDa exclusion size membrane (Millipore, Bedford, USA).

Enzyme Activity Assay

Fifty microliters of an enzyme solution were added to 950 μl of a 4 or 8 mM pnpR solution (in sodium acetate buffer, pH 5.5) in a plastic cuvette at 60 °C. The final protein concentration in the cuvette was 0.6–2 mg l^{-1} for Naringinase solutions, 2 mg l^{-1} for enriched enzyme solutions, and 0.45–36 mg l^{-1} for pooled fraction after column treatment. The increase of *p*-nitrophenolate (pnp) concentration was followed by monitoring the absorption at 400 nm (molar absorption coefficient for pnp: 1.17 l $mmol^{-1}$ cm^{-1} at pH 5.5 and 60 °C) during 5 min reaction time in a photometer provided with a heated cell changer (Amersham Biosciences) and coupled to the software Swift II reaction kinetics (Biochrom, Cambridge, UK). One unit was defined as the protein amount that converts 1 μmol pnp from pnpR in 1 min at 60 °C and pH 5.5. Activity assays for stability tests were performed by double determinations with 8 mM pnpR solution in 0.5 M sodium acetate buffer, whereas simple determinations at 4 mM pnpR solution in 0.1 M sodium acetate buffer were carried out for activity assays of pooled fractions after enrichment.

Protein Determination

The protein concentration of collected fractions from α-L-rhamnosidase enrichments were determined by the Bradford method [26] (Bio-Rad Laboratories, Munich, Germany) using BSA as standard.

Response Surface Methodology

The experimental design methodology [27–30] was used for studying the stability of Naringinase. This methodology is based on multivariate methods where the levels (settings or values) of the independent variables (e.g., processing conditions, X_i) are simultaneously modified from one experiment to another. These methods find their major application when the effect of one variable is affected by the setting of another one. Such "interaction effects" between variables are difficult to detect by a traditional experimental setup where one variable is changed at a time. The experimental design methodology makes use of statistical tools for selecting a minimum set of experiments adequately distributed in the experimental region (experimental matrix). These experiments are chosen so that the coefficients of the mathematical model (usually a polynomial equation) representing the variations of the experimental response of interest [dependent variable $Y=f(X_i)$] may be evaluated with the best possible precision. The least-square estimates of the coefficients of the model (b_j) are calculated from the values of the response y for each experiment in the chosen experimental matrix. The resulting model allows the drawing of contour plots (lines or curves of constant response value) and of three-dimensional representations of the responses (response surface methodology) [29, 31–33]. Once tested, the model may be used to predict the value of the response(s) under any conditions within the experimental region.

Model Selection

Due to the complexity of the events involved in protein inactivation, the dependency of the responses on the variables were not expected to be linear, the experimental responses were therefore fitted to an empirical quadratic polynomial model of the form:

$$Y = b_0 + \sum b_i \cdot X_i + \sum b_{ii} \cdot X_i^2 + \sum \sum b_{ij} \cdot X_i \cdot X_j \quad (1)$$

In Eq. 1, b_0 is the average of all experimental responses, b_i the main effect coefficient of the variable X_i, b_{ii} the second-order effect coefficient of the variable X_i, and b_{ij} the interaction effect coefficient between variables X_i and X_j ($i \neq j$).

Experimental Design

Among all possible experimental designs associated to a quadratic model [27–30], a Doehlert array was selected for two reasons: Besides providing a uniform array of optimally selected experiments within the experimental region, it allows a stepwise approach, investigating in a first step the influence of two variables and extending then the treatment to more variables [31–34]. In the first step, a Doehlert matrix for two variables was used for investigating the temperature and pH effects. This matrix contains seven uniformly distributed experiments (Table 1, experiments 1–7) that may be represented in normalized variables (X_i) by the apexes and the center of a hexagon. In a second step, a third variable

Table 1 Doehlert array of experiments for three variables.

Exp. no.	pH Value		Temperature		Enzyme concentration	
	Coded	Effective (−)	Coded	Effective (°C)	Coded	Effective (g/l)
Experimental matrix for temperature and pH						
1	+1.0000	6.00	0	65	0	0.525
2	−1.0000	2.50	0	65	0	0.525
3	+0.5000	5.13	+0.8660	78	0	0.525
4	−0.5000	5.13	−0.8660	52	0	0.525
5	+0.5000	3.38	−0.8660	52	0	0.525
6	−0.5000	3.38	+0.8660	78	0	0.525
7	0	4.25	0	65	0	0.525
Extended matrix for coupling of enzyme concentration						
8	+0.5000	5.13	+0.2887	69	+0.8165	0.913
9	−0.5000	3.38	−0.2887	61	−0.8165	0.137
10	+0.5000	5.13	−0.2887	61	−0.8165	0.137
11	0	4.25	+0.5774	74	−0.8165	0.137
12	−0.5000	3.38	+0.2887	69	+0.8165	0.913
13	0	4.25	−0.5774	56	+0.8165	0.913
Repetitions at the center of the experimental region						
14 to 18	0	4.25	0	65	0	0.525
Control experiments						
A	0.1400	4.50	−0.3300	60	0	0.525
B	0.5000	5.13	0	65	0	0.525

Set of variable-levels: temperature at seven levels, pH value at five levels, and Naringinase concentration at three levels.

(enzyme concentration) was introduced by adding six experiments (Table 1, experiments 8–13), resulting in a matrix containing 13 experiments that may be represented by the apexes and center of a cube octahedron [33].

Determination of the Experimental Region

Considering the application of the Naringinase for biotransformation of rhamnolipids, the range of each variable was determined according to possible process conditions. The temperature range was selected from 50 to 80 °C, the pH value was set between 2.5 and 6.0, and the Naringinase concentration between 0.1 and 1 g l^{-1}. Because different variables have different units and ranges of variation, the value of the variables are coded or normalized as: $X_i = (U_i - U_0)/\Delta U$, where X_i is the normalized variable (range from −1 to +1), U_i the value of the effective variable, U_0 the value at the center of the variable range, and ΔU_i the step $\left(= \left(U_{i,\max} - U_{i,\min}\right)/2\right)$. Table 1 lists the series of experiments in normalized and effective variables.

The reproducibility of the experimental responses was determined by five repetitions of the experiment at the center of the experimental region (all variables at normalized value 0). The fitting of the stability curves to the proposed deactivation model and also of initial pnpR activities to the Michaelis–Menten equation was made by the least-square regression method using the Levenberg–Marquardt algorithm (Sigma plot 9.01, Systat software, Inc., San Jose, USA). The calculation of the enzyme half-life values from the activities–time expression was carried out with the program Mathcad 13 (Mathsoft® Needham, USA). For

building the experimental matrices, calculating the coefficients of the model (Eq. 1), evaluating the significance of regression, and performing the validity tests, the NEMROD program was used [34].

Results

Kinetics of α-L-Rhamnosidase at Assay Conditions

For establishing the activity assay, the kinetic parameters of the conversion of pnpR by α-L-rhamnosidase were determined at 60 °C and pH 5.5 in 0.1 M sodium acetate by measurement of the initial reaction rate at different initial pnpR concentrations. After fitting the data to the Michaelis–Menten equation, the maximal specific activity and the Michaelis–Menten constant (K_M) were evaluated to be 13.3±0.4 U mg^{-1} (relative to powder amount) and 6.1±0.3 mM, respectively. Product effects like backward reactions and inhibition phenomena were not considered, since initial reaction rates were taken for the calculation. The K_M value thus obtained was higher than the one reported by Romero et al. [3] at pH 3.5 (1.52 mM), and therefore, a higher initial pnpR concentration was used for greater accuracy in the activity assays.

Stability at Low Naringinase Concentration

First, stability assays were performed at low enzyme powder concentration (0.01 g l^{-1}) resembling the conditions of rhamnolipid activity assays. In the temperature range from 40 to 60 °C, the activity rapidly decreased within the first 30 min incubation time but afterwards remained constant at about 45% of the initial value for 5 h (data not shown). Incubation without agitation caused a similar behavior, but the remaining activity after 30 min was higher (80% of the initial value). Ellenrieder and Daz [5] found thermostabilization of naringinase by the presence of BSA. Therefore, 1 g l^{-1} BSA was added to the incubation buffer, and the rapid activity decrease within the first 30 min was no longer observed. The activity remained constant and equal to the initial value until 5 h. Moreover, this decay was gradually reduced with higher enzyme concentrations, completely disappearing at 0.1 g l^{-1} Naringinase powder concentration and indicating subunit dissociation. However, when handling with very dilute enzyme solutions, a significant percentage of protein can be adsorbed on the walls of the incubation vessel accounting for the former observations [35]. To detect this, stability assays at a concentration of 0.01 g l^{-1} Naringinase were performed in pre-treated vessels with BSA or Naringinase absorbed on their surfaces [36]. The apparent deactivation at the beginning was hereby no longer observed. The lower limit of the variable enzyme concentration was therefore set up to 0.1 g l^{-1} for the response surface study to avoid adsorption of a high percentage of protein on the vessel walls.

Proposed Deactivation Model

Figure 1 shows the decreasing activity as a function of time at different conditions of temperature and pH values. In a half-logarithmic diagram, a non-linear behavior between time and residual activity is observed for all cases. The decay of the first part of the curve is more pronounced than the second part. Actually, for all experiments carried out for the response surface analysis, it was not possible to fit acceptably the experimental data to the

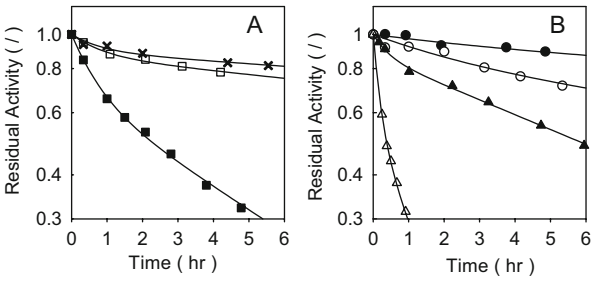

Fig. 1 Stability of Naringinase at different conditions. **A** Effect of pH value on enzyme stability at 65 °C: pH 4.25 (*crosses*); pH 6.00 (*white squares*); pH 2.50 (*black squares*). **B** Effect of temperature on enzyme stability at pH 3.38; 52 °C (*black circles*); 61 °C (*white circles*); 69 °C (*black triangles*); 78 °C (*white triangles*)

common single-exponential decay. However, for all conditions, an adequate fitting to a two-exponential equation of the form [25],

$$a = C_1 \cdot e^{-q_1 t} + (1 - C_1) \cdot e^{-q_2 t} \tag{2}$$

could be achieved. In Eq. 2, a is the normalized residual activity related to the initial value and C_1, q_1, and q_2 are the equation parameters, which can be evaluated by the fitting. This multiple-exponential behavior in the stability curve is always observed when more than one independent, potentially active form of the enzyme is involved on the deactivation kinetics [25]. As with single-exponential decay, a certain number of possible deactivation mechanisms could be applied to explain the double-exponential behavior. However, the values of the physical parameters of the mechanism can only be determined from deactivation data when the number of equation parameters equals the number of the physical ones. Otherwise, the parameters are evaluated as "lumped" or as apparent rate constants of a more complicated mechanism [25]. Therefore, double-exponential deactivation behavior is often explained by the most simple series type mechanism: the initial enzyme form (E) first deactivates to a still active intermediate state (E_1), which slower deactivates to the final fully inactivated state (E_d):

$$E \xrightarrow{k_1} \overset{\beta_1}{E_1} \xrightarrow{k_2} E_d \tag{3}$$

In Eq. 3, β_1 is the specific activity of the intermediate state E_1 related to the initial state (E), and k_1 and k_2 are the respective rate constants of the first and second deactivation reactions. Assuming that these steps are irreversible, the second rate constant k_2 is equal to the parameter q_2 from Eq. 2. Further assuming that no parallel reactions from E to E_d take place and that only the form E is present at the initial state, the activity–time expression corresponding to the former deactivation equation is [25]:

$$a = \left(1 + \frac{\beta_1 \cdot k_1}{k_2 - k_1}\right) e^{-k1t} - \frac{\beta_1 \cdot k_1}{k_2 - k_1} e^{-k2t} \tag{4}$$

Comparing Eqs. 2 and 4, the value of the physical parameters β_1, k_1, and k_2 can be then evaluated from the equation parameters C_1, q_1, and q_2. The physical parameters were then taken as responses for the experiments (Doehlert matrix). Moreover, when a equals 0.5, a half-life value ($t_{1/2}$) can be calculated from Eq. 2 and can be taken as a further response as well.

Response Surface Analysis

The experimental responses β_1, k_1, k_2, and $t_{1/2}$ of every stability assay under defined incubation conditions according to the corresponding Doehlert array (Table 1) are

summarized in Table 2. In all cases, the rate constant k_1 was higher than the second rate constant k_2, which agrees with the proposed deactivation model. However, as can be seen from the repeated experiments at the center, the standard deviation (s) of the response k_1 was rather high compared with the s of the other responses. Probably, more experimental points at the very beginning of the stability assays could have been required for measuring this rapid deactivation decay with acceptable accuracy. Therefore, this response was not taken into account for the analysis. Taking the first experiments 1 to 7 and the center repetitions 14 to 18 and by multiple regressions analysis of the responses k_2 ($\log k_2$) and β_1, polynomial models were obtained at constant Naringinase concentration (0.525 g l^{-1}). The coefficients of the models are given in Eqs. 5 and 6, respectively. In these equations, X_1 and X_2 represent the normalized variables for pH and temperature, respectively.

$$\log(k_2) = -1.85_{(\pm 0.03)} - 0.47_{(\pm 0.04)}X_1 - 1.11_{(\pm 0.04)}X_2 + 0.67_{(\pm 0.05)}X_1^2 + 0.42_{(\pm 0.05)}X_2^2 + 0.23_{(\pm 0.08)}X_1X_2 \quad (5)$$

Table 2 Responses of the experimental matrix assays.

Exp. no.	$k_1 \times 10^2$ (h^{-1})	$k_2 \times 10^2$ (h^{-1})		β_1 (/)		$t_{1/2}$ (h)	
	Exp[a]	Exp[a]	Calc[b]	Exp[a]	Calc[b]	Exp[a]	Calc[b]
1	127	2.5	2.2	0.86	0.89	23	26
2	205	17.4	19.2	0.68	0.65	2.3	2.0
3	482	25.7	28.4	0.71	0.68	1.6	1.4
4	93.6	0.2	0.2	0.92	0.89	309	268
5	20.8	1.1	1.0	0.85	0.88	52	61
6	408	58.9	53.3	0.44	0.47	0.40	0.46
8	78.2	2.9	3.2 (2.9)	0.75	0.77 (0.84)	16	15 (18)
9	31.5	3.0	2.6 (2.0)	0.73	0.71 (0.83)	16	18 (27)
10	116	0.7	0.8 (0.6)	0.86	0.91 (0.91)	78	84 (105)
11	170	8.9	9.5 (8.5)	0.76	0.72 (0.70)	5.3	4.5 (4.7)
12	13.1	9.5	9.1 (7.5)	0.83	0.78 (0.69)	5.8	5.3 (5.3)
13	254	0.5	0.5 (0.5)	0.92	0.96 (0.91)	120	141 (138)
Control experiments							
A	52.0	0.3	0.6	0.86	0.91	165	103
B	118	1.5	1.2	0.88	0.89	38	48
Repetitions at the centre of the experimental region							
7	118	1.6		0.88		36	
14	290	1.7		0.92		36	
15	309	1.3		0.82		38	
16	442	1.3		0.81		37	
17	530	1.3		0.82		39	
18	70.0	1.3		0.86		44	
Average	293	1.4		0.85		38	
s[c]	178	0.2		0.04		3	

[a] Experimental responses

[b] Response calculated by the corresponding prediction model: Eqs. 5 and 6 for experiments 1–6 and Eqs. 7 and 8 for experiments 8–13. In parenthesis, the calculated values from pH–temperature prediction model (Eqs. 5 and 6)

[c] Standard deviation of the experimental response

$$\beta_1 = 0.85_{(\pm 0.02)} + 0.12_{(\pm 0.03)}X_1 - 0.18_{(\pm 0.03)}X_2 - 0.08_{(\pm 0.04)}X_1^2 - 0.14_{(\pm 0.04)}X_2^2 + 0.12_{(\pm 0.06)}X_1X_2 \quad (6)$$

The standard deviations of the responses are 0.07 and 0.05 for $\log k_2$ and β_1, respectively. The multiple regression coefficients R^2 are equal to 0.995 (R^2 adjusted of 0.991) for $\log k_2$ and 0.932 (R^2 adjusted of 0.873) for β_1. The results of F tests have shown that the polynomial regressions are statistically significant at a confidence level higher than 95% (F=241.8 for $\log(k_2)$ response and F=16.1 for β_1 response; $F_{5\%}(5;6)$=4.39); indeed, the chosen variables affect significantly the experimental responses (Table 2). The good agreements between experimental and calculated values (Table 2) confirm the validity of the polynomial models obtained (Eqs. 5 and 6). The experimental responses of the control assays, shown also in Table 2, are in agreement with the calculated values from the model equations within experimental error. From a practical point of view, it could be interesting also to predict the value of the half-life of the enzyme under given process conditions. Taking the logarithm value of $t_{1/2}$, an empirical quadratic model for this response could be calculated as shown in Eq. 7:

$$\log(t_{1/2}) = 1.58_{(\pm 0.01)} + 0.56_{(\pm 0.02)}X_1 - 1.27_{(\pm 0.02)}X_2 - 0.72_{(\pm 0.03)}X_1^2 - 0.53_{(\pm 0.03)}X_2^2 - 0.10_{(\pm 0.04)}X_1X_2 \quad (7)$$

Figure 2 shows the three-dimensional representation and the contour plots of the prediction models for $\log(k_2)$, β_1, and $t_{1/2}$. To display the direct value of half-life, Eq. 7 was plotted in Fig. 2 after solving it for $t_{1/2}$. The prediction model for $\log(k_2)$ shows that k_2 decreases with decreasing temperature, indicating as expected, an increasing stability at

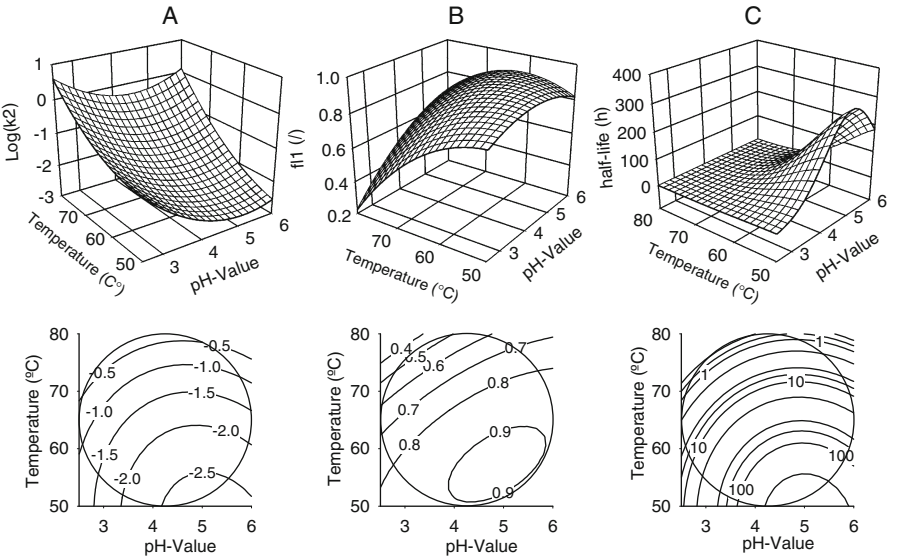

Fig. 2 Three dimensional representation of the response surfaces for $\log(k_2)$ (**A**), β_1 (**B**), and half-life (**C**). The corresponding contour plots are plotted under each response surfaces (the *circle* denotes the experimental region)

lower temperatures. The k_2 value also depends on the pH, and this behavior varies with the temperature reflecting the contribution of the interaction coefficient in Eq. 5. The model parameter β_1 ranged from 0.25 to 0.90 suggesting that the intermediate state E_1 is less active than the initial state for all conditions. Hereby, the higher the incubation temperature, the lower the activity of the intermediate state, and this dependency is also influenced by the incubation pH. Variations of the β_1 value with pH were already observed with glucose phosphate isomerase [25].

For extending the analysis to the third variable, Naringinase concentration, experiments 8–13 (Table 1) were carried out and then the coefficients of the corresponding models for three variables (experiments 1–17) were calculated by multiple regression analysis and are given in Eqs. 8 and 9. In these equations, X_1, X_2, and X_3 represent the normalized variables for pH, temperature, and Naringinase concentration, respectively.

$$\begin{aligned}\log(k_2) = {} & -1.85_{(\pm 0.03)} - 0.49_{(\pm 0.03)}X_1 + 1.09_{(\pm 0.03)}X_2 - 0.03_{(\pm 0.03)}X_3 \\ & + 0.67_{(\pm 0.06)}X_1^2 + 0.42_{(\pm 0.06)}X_2^2 + 0.11_{(\pm 0.05)}X_3^2 + 0.23_{(\pm 0.08)}X_1X_2 \\ & - 0.03_{(\pm 0.09)}X_1X_3 + 0.07_{(\pm 0.09)}X_2X_3 \end{aligned} \tag{8}$$

$$\begin{aligned}\beta_1 = {} & 0.85_{(\pm 0.02)} + 0.09_{(\pm 0.03)}X_1 - 0.16_{(\pm 0.03)}X_2 + 0.03_{(\pm 0.03)}X_3 - 0.08_{(\pm 0.05)}X_1^2 \\ & - 0.14_{(\pm 0.05)}X_2^2 - 0.01_{(\pm 0.04)}X_3^2 + 0.12_{(\pm 0.07)}X_1X_2 - 0.17_{(\pm 0.07)}X_1X_3 \\ & - 0.09_{(\pm 0.07)}X_2X_3 \end{aligned} \tag{9}$$

From the new polynomial models for both responses, it was clearly observed that almost all coefficients involving the enzyme concentration variable (X_3) were much lower than the other coefficients and of the order of their standard deviations and are therefore evaluated as non-significant. This observation indicates that this variable and its interactions hardly influence the Naringinase stability ($\log k_2$ value) or the specific activity of its intermediate state (β_1 value) within the tested region (0.1–1 g l^{-1} Naringinase powder concentration). As can be observed from Table 2, experimental and predicted values from Eqs. 5, 6, and 7 (values in parentheses) for the six complementary experiments are in acceptable agreement within experimental error confirming the former assumption.

Enrichment of α-L-Rhamnosidase and its Stability

Since the commercial preparation used seems to be a raw powder of only 7.8% *w*/*w* protein content (according to Bradford) containing foreign proteins of lower molecular weights (data not shown), it can be worthwhile to perform incubation experiments with a more purified α-rhamnosidase to support the above observations. Activity was eluted in two peaks from an anion adsorbent, one portion eluting before the elution buffer was applied and a later peak together with unwanted proteins. A shift of the second activity peak into the first one was achieved by lowering the pH of the buffer system. The activity recovery in the first peak was then increased from 66% at pH 7.5 to 70% at pH 7.0 and 93% for pH 6.5. Figure 3 shows a typical chromatogram under optimal conditions. At large scale, a partial purification of Naringinase was achieved. The enzyme concentrate of the pooled fractions resulted in a 2.8-fold increase in specific activity with 82% activity recovery. The specific protein activity of the initial sample was 52.5 U mg^{-1} and of the enriched enzyme 148 U mg^{-1}.

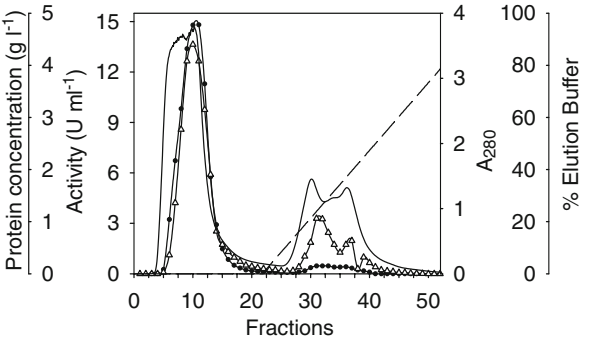

Fig. 3 Anion exchange chromatography of Naringinase on Hitrap-Q-FF. *Black circles* Rhamnosidase activity; *white triangles* protein concentration; *full line* absorption at 280 nm and; *dashed line*, percentage of elution buffer in the running buffer

Stability studies of the enriched α-L-rhamnosidase under different temperature and pH values were carried out. For all conditions tested, it was again not possible to fit the experimental points to the common exponential deactivation. However, the data could be appropriately fitted to the proposed double exponential mechanism. Table 3 gives the values of the parameters k_1, k_2, and β_1 for the conditions tested. These values agree with the values predicted by the models (Eqs. 5 and 6) for deactivation of the unpurified α-L-rhamnosidase (Naringinase), and it can therefore be concluded that: (1) the enriched enzyme is as stable as the mixed unpurified powder and (2) any influence of low molecular weight substances (e.g., additives, contaminants, or stabilizers) on the enzyme stability was negligible.

Discussion

Many examples of soluble, immobilized, and chemically modified enzymes exhibiting series-type deactivation mechanism are available in the literature [9, 25, 37, 38]. Moreover, Soria and Ellenrieder [9] also proposed a series-type mechanism for thermal deactivation of a α-L-rhamnosidase of *Aspergillus terreus*. Although there is no evidence at a molecular level of the formation of an intermediate state during deactivation, some valuable insights were gained to suggest that the proposed model may apply: First, the incubation conditions are similar for obtaining lower deactivation constants (k_2) and greater activity of the intermediate state (β_1), which both promote greater enzyme stabilities. This indicates congruent tendencies. Moreover, the enriched enzyme also exhibited series-type deactivation kinetics supporting the assumption that the deactivation mechanism may be an intrinsic characteristic of the enzyme.

Gabor and Pittner [17] reported that Naringinase tends to self-digest, cleaving 160–170 mol of glucose per mole of enzyme and being, in this digested state, less active and less

Table 3 Responses of the stability assays of the purified α-L-rhamnosidase.

Temperature (°C)	pH Value (–)	$k_1 \times 10^2$ (h^{-1})	$k_2 \times 10^2$ (h^{-1})	β_1 (–)	$t_{1/2}$ (h)
60	4.50	438	0.6 (0.6)	0.95 (0.91)	116 (103)
61	5.13	50.3	0.8 (0.6)	0.89 (0.91)	72 (105)
65	5.13	32.6	1.2 (1.2)	0.82 (0.89)	46 (48)
78	5.13	503	36.8 (28.4)	0.74 (0.68)	1.3 (1.4)

In parentheses, the calculated values with non-purified enzyme (Naringinase) from Eqs. 5 and 6

stable. In account of this, the first faster deactivation step observed may correspond to the unfolding and self-digestion of the carbohydrate portion, lowering its activity relative to the initial state (β_1); afterwards, the common phenomena involving enzyme inactivation may apply for the second slower step. The digestion and unfolding grade of this intermediate state may also be controlled by the pH and temperature of incubation.

On the other hand, elution from the Q-column in two activity peaks may indicate existence of α-L-rhamnosidases with different grade of glycosidation having different affinity to the matrix, or even coexistence of different enzymes molecules with different active centers. However, sodium dodecyl sulfate page revealed protein bands at about 90 kDa for both fractions (data not shown). Mutter et al. [6] and Manzanares et al. [7] detected two different α-L-rhamnosidase activities from *Aspergillus aculeatus.* Young et al. [4] reported purification of *P. decumbens* α-rhamnosidase in a Mono Q column. They also observed activity elution in two peaks; however, the adsorption onto the column was stronger, since at pH 6.0, the major peak was still the later one coming together with the β-glucosidase portion. The observed double exponential deactivation kinetics may be explained in this case by a stability profile resulting from the contributions of the different deactivation mechanism of the two species.

Concerning stability data, it can be concluded that (1) the glycol-enzyme is a rather thermo-stable enzyme preserving its initial activity for long times when incubated at its optimal pH up to temperatures of 65 °C; (2) the stability of the enzyme is insensitive to the enzyme concentration; (3) a pH-optimum for enzyme stability could be observed at pH 4.5–5.0 by analysis of the response surfaces at constant temperature being, however, quite sensitive to lower pHs (<3.5). Ellenrieder and Daz [5] and Tsen et al. [19] reported deactivation data of *Penicillium* Naringinase at pH 3.5–3.7; however, our measurements exhibited higher stability at the same conditions. Ellenrieder and Daz [5] also observed an increasing stability at higher Naringinase concentrations; however, the range tested by these authors was wider (0.5–5 g l^{-1}). They also achieved thermo-stabilization by cross-linking modification and by immobilization on protein-rich supports. Many studies of pH-stability on *Aspergillus* rhamnosidases are reported [1, 6–9, 13, 14]. *A. aculeatus* α-L-rhamnosidase [6] was shown to be insensitive to pH in the range 3–8, whereas *A. terreus* [8] and *Aspergillus nidulans* [14] α-L-rhamnosidases rapidly lost activity when incubated at pH values lower than 4.0. Comparing our measurements with available stability data of purified fungal α-L-rhamnosidases published in the literature [1, 6–9, 13, 14], it can be further pointed out that α-L-rhamnosidase from *P. decumbens* exhibited higher thermo-stability than from *Aspergillus* species.

Response surface methodology has been successfully applied for the quantitative study of enzyme stability. Compared to the traditional approach consisting of changing one variable at a time, response surface methodology significantly reduced experimental effort and facilitated data treatment and interpretation of the results. Thus, temperature, pH, and enzyme concentration effect on stability were evaluated on a minimum set of optimal selected experiments. Estimations of deactivation parameters at different conditions were chosen as responses for every experiment. With these responses, an empirical quadratic model was fitted for predicting enzyme stability within the experimental region serving as a basis for a rational selection of conditions of Naringinase catalysed reactions like, e.g., rhamnolipid hydrolysis. Further investigations for establishing coexistence of different enzymes molecules in Naringinase, e.g., by measuring eluted activity with two different substrates from a purification column supported by stability profiles of the different activity peaks, are being planned. In case of detection of two different enzymes, the proposed series deactivation mechanism should be re-evaluated.

Acknowledgments The authors would like to thank the financial support of this project, carried out in the framework of a EU-CRAFT project (1999-72243) entitled "Integrated process for bio-surfactant synthesis at competitive cost allowing for their application in household cleaning and bio-remediation" (InBioSynAp). We also thank Rebecca Lorenz for her helpful practical input during the research project.

References

1. Dunlap, W. J., Hagen, R. E., & Wender, S. H. (1962). *Journal of Food Science*, *27*(6), 597.
2. Puri, M., & Banerjee, U. C. (2000). *Biotechnology Advances*, *18*(3), 207–217.
3. Romero, C., et al. (1985). *Analytical Biochemistry*, *149*(2), 566–571.
4. Young, N. M., Johnston, R. A. Z., & Richards, J. C. (1989). *Carbohydrate Research*, *191*(1), 53–62.
5. Ellenrieder, G., & Daz, M. (1996). *Biocatalysis and Biotransformation*, *14*(2), 113–123.
6. Mutter, M., et al. (1994). *Plant Physiology*, *106*(1), 241–250.
7. Manzanares, P., et al. (2001). *Applied and Environmental Microbiology*, *67*(5), 2230–2234.
8. Gallego, M. V., et al. (2001). *Journal of Food Science*, *66*(2), 204–209.
9. Soria, F., & Ellenrieder, G. (2002). *Bioscience Biotechnology and Biochemistry*, *66*(7), 1442–1449.
10. Meiwess, J., Wullbrant, D., & Giani, C. (1994) EP0599159.
11. Trummler, K., Effenberger, F., & Syldatk, C. (2003). *European Journal of Lipid Science and Technology*, *105*(10), 563–571.
12. Mamma, D., et al. (2004). *Food Biotechnology*, *18*(1), 1–18.
13. Manzanares, P., de Graaff, L. H., & Visser, J. (1997). *FEMS Microbiology Letters*, *157*(2), 279–283.
14. Manzanares, P., et al. (2000). *Letters in Applied Microbiology*, *31*(3), 198–202.
15. Monti, D., et al. (2004). *Biotechnology and Bioengineering*, *87*(6), 763–771.
16. Scaroni, E., et al. (2002). *Letters in Applied Microbiology*, *34*(6), 461–465.
17. Gabor, F., & Pittner, F. (1984). *Hoppe-Seylers Zeitschrift Fur Physiologische Chemie*, *365*(9), 914–914.
18. Turecek, P., & Pittner, F. (1986). *Applied Biochemistry and Biotechnology*, *13*(1), 1–13.
19. Tsen, H. Y., Tsai, S. Y., & Yu, G. K. (1989). *Journal of Fermentation and Bioengineering*, *67*(3), 186–189.
20. Puri, M., Marwaha, S. S., & Kothari, R. M. (1996). *Enzyme and Microbial Technology*, *18*(4), 281–285.
21. Norouzian, D., et al. (1999). *World Journal of Microbiology & Biotechnology*, *15*(4), 501–502.
22. Biselli, M., Krugl, U., & Wandrey, C. (1995). In K. Drauz, & H. Waldman (Eds.), *Enzyme catalysis in organic synthesis—a comprehensive handbook, Vol. 1* (pp. 89–155). Weinheim: VCH.
23. Klibanov, A. M. (1983). *Advances in Applied Microbiology*, *29*, 1–28.
24. Bisswanger, H. (1999). *Enzymkinetik: Theorie und methoden* (3rd ed.). Weinheim: Wiley-VCH.
25. Sadana, A. (1991). *Biocatalysis: Fundamentals of enzyme deactivation kinetics*. New Jersey: Prentice Hall.
26. Bradford, M. M. (1976). *Analytical Biochemistry*, *72*(1–2), 248–254.
27. Aktinson, C. (1992). *Optimum experimental designs*. Oxford: Clarendon.
28. Box, G. E. P., Hunter, W. G., & Hunter, J. S. (1978). *Statistic for experimenters: An introduction to design, data analysis and model building*. New York: Wiley.
29. Khuri, A. I., & Cornell, J. A. (1987). *Response surfaces, design and analyses*. New York: Marcel Dekker.
30. Rasch, D., Verdooren, L. R., & Gowers, J. I. (1999). Grundlagen der Planung und Auswertung von Versuchen und Erhebungen, R. Oldenbourg Verlag, München, Wien
31. BenoitMarquie, F., et al. (1997). *Journal of Photochemistry and Photobiology A—Chemistry*, *108*(1), 65–71.
32. Oliveros, E., et al. (2000). In *Proceedings of the third Asia pacific conference* (pp. 577–581). Singapore, Work Scientific.
33. Oliveros, E., et al. (1997). *Chemical Engineering and Processing*, *36*(5), 397–405.
34. NEMRODW LPRAI, B.P. no. 7, Marseille - Le Merlan, 13311 Marseille Cedex 14, France. Retrieved from www.nemrodw.com.
35. Scopes, R. (1994). *Protein purification, principles and practice* (3rd ed.). New York: Springer.
36. Mozhaev, V. V. (1993). *Trends in Biotechnology*, *11*(3), 88–95.
37. Greco, G., et al. (1992). In *Stability and stabilization of enzymes (Proceedings of an International Symposium)* (pp. 429–435). Maastricht: Elsevier Science.
38. Prazeres, D. M. F., Garcia, F. A. P., & Cabral, J.M. S. (1992). In *Stability and stabilization of enzymes (Proceedings of an International Symposium)* (pp. 445–450). Maastricht: Elsevier Science.